Eur. J. Biochem. **269**, 5642–5648 (2002) © FEBS 2002 doi:10.1046/j.1432-1033.2002.03271.x

Solution structure of the Alzheimer amyloid β-peptide (1–42) in an apolar microenvironment

Similarity with a virus fusion domain

Orlando Crescenzi[1], Simona Tomaselli[1], Remo Guerrini[2], Severo Salvadori[2], Anna M. D'Ursi[3], Piero Andrea Temussi[1] and Delia Picone[1]

[1]*Dipartimento di Chimica, Università degli Studi di Napoli 'Federico II', Italy;* [2]*Dipartimento di Scienze Farmaceutiche, Università di Ferrara, Italy;* [3]*Dipartimento di Scienze Farmaceutiche, Università di Salerno, Italy*

The major components of neuritic plaques found in Alzheimer disease (AD) are peptides known as amyloid β-peptides (Aβ), which derive from the proteolitic cleavage of the amyloid precursor proteins. *In vitro* Aβ may undergo a conformational transition from a soluble form to aggregated, fibrillary β-sheet structures, which seem to be neurotoxic. Alternatively, it has been suggested that an α-helical form can be involved in a process of membrane poration, which would then trigger cellular death.

Conformational studies on these peptides in aqueous solution are complicated by their tendency to aggregate, and only recently NMR structures of Aβ-(1–40) and Aβ-(1–42) have been determined in aqueous trifluoroethanol or in SDS micelles. All these studies hint to the presence of two helical regions, connected through a flexible kink, but it proved difficult to determine the length and position of the helical stretches with accuracy and, most of all, to ascertain whether the kink region has a preferred conformation. In the search for a medium which could allow a more accurate structure determination, we performed an exhaustive solvent scan that showed a high propensity of Aβ-(1–42) to adopt helical conformations in aqueous solutions of fluorinated alcohols. The 3D NMR structure of Aβ-(1–42) shows two helical regions encompassing residues 8–25 and 28–38, connected by a regular type I β-turn. The surprising similarity of this structure, as well as the sequence of the C-terminal moiety, with those of the fusion domain of influenza hemagglutinin suggests a direct mechanism of neurotoxicity.

Keywords: Alzheimer disease; amyloid peptides; conformational analysis; fusion domain; NMR.

Alzheimer disease (AD), the well known neurodegenerative disorder associated with neuronal loss, is at present one of the most studied pathologies; nevertheless, it is still one of the least understood at the molecular level.

The brains of AD patients are characterized by extracellular proteic plaques and intracellular neurofibrillary tangles [1]. Plaques are built up by fibrils whose major component are peptides known as β-amyloid (Aβ), which range in length from 39 to 43 amino acids. All of them have a great propensity towards aggregation in aqueous solution, but the major form found in plaques is Aβ-(1–42). The relative abundance of Aβ-(1–42) with respect to Aβ-(1–40) reflects the fact that even a small elongation of the stretch of hydrophobic residues in the C-terminal region increases dramatically the tendency of this peptide to aggregate [2].

Correspondence to D. Picone, Dipartimento di Chimica, Università degli Studi di Napoli 'Federico II', via Cintia 26, Complesso Universitario di Monte S. Angelo, 80126 Napoli, Italy.
Fax: + 39 081 674409, Tel.: + 39 081 674406,
E-mail: picone@chemistry.unina.it

Abbreviations: AD, Alzheimer disease; Aβ, amyloid beta-peptides; Aβ-(1–40), amyloid beta-peptide 1–40; Aβ-(1–42), amyloid beta-peptide 1–42; APP, amyloid precursor protein; HA_fd, fusion domain of influenza hemagglutinin; HFIP, hexafluoroisopropanol.

(Received 18 July 2002, revised 16 September 2002, accepted 19 September 2002)

Amyloid peptides originate from cleavage of a common precursor called amyloid precursor protein (APP) [3], a glycoprotein of 695–770 amino acids which comprises three parts: the extracellular N-terminal region, a single hydrophobic transmembrane region and the cytoplasmic C-terminal domain. As the genes encoding APP are on chromosome 21, individuals affected by Down's syndrome overexpress APP and may develop early AD forms [4].

APP can be cleaved proteolitically by different proteases, called α, β and γ secretases [5]. The α secretase cleaves APP within the Aβ sequence, and its products are not neurotoxic. Alternatively, APP can be hydrolyzed by the β secretase activity at the N-terminus of Aβ, which is successively released by the γ secretase after cleavage within the membrane [6] either between residues 40 and 41 or between residues 42 and 43. Thus, the N-terminal region of Aβ-(1–42) derives from the extracellular domain of the precursor, whereas its C-terminal region derives from the membrane-spanning domain [7].

It is generally recognized that the presence of fibrils is necessary for toxicity [8] but it is not generally agreed whether toxicity is generically linked to the occupation of a large area of the cell surface or there is a direct action upon the cell membrane. A possible explanation of the peptide neurotoxicity invokes, as the key event, a membrane-poration process. According to this view, which is supported by the results of *in vitro* electrophysiologic measurements, the α-helical conformation of the peptide would induce formation of membrane channels, allowing the penetration

of substances (such as metal ions) which can cause neuronal death [9,10]. At any rate, both views evidence a critical role for *in vivo* conformational transitions involving soluble forms of the peptide. As a matter of fact, previous solution studies evidenced that Aβ can indeed assume different conformations even *in vitro*, depending on the experimental conditions. Thus, for example, it has been recently reported that the fibrillogenesis process of Aβ-(1–40) and Aβ-(1–42) involves an oligomeric α-helical intermediate [11].

Several NMR measurements on both Aβ-(1–40) and Aβ-(1–42) have been carried out in different solvents mimicking the interface between aqueous and apolar phases, such as SDS micelles [12,13] and in solvents that can reproduce an apolar microenvironment, such as trifluoroethanol/water mixtures [14].

All these studies evidenced the presence of two helical regions, connected by a more flexible and disordered link; however, there is no consensus on the length and position of the helical stretches nor on the structural features of the link region. Another point that should be considered is the complex heterogeneous nature of SDS solutions, which does not necessarily reflect the conformational tendencies in a physiological apolar environment (such as the lipid phase of membranes). Moreover, the very role played by the micellar environment is not generally agreed on: thus, Coles *et al*. [12] suggested that the α-helical region might correspond to the portion of the peptide crossing the membrane, whereas Shao *et al*. [13] reported evidence that the peptide is located entirely on the outside of the micelles, in contact with the negatively charged surface.

In this paper we report on a CD and 2D NMR conformational study of Aβ-(1–42) in several media that can create apolar microenvironments mimicking the lipid phase of membranes. The most detailed structure was obtained using aqueous mixtures of a fluorinated alcohol, hexafluoroisopropanol (HFIP). HFIP has been chosen as a result of a vast exploratory search because it can dissolve Aβ-(1–42) better than all other media and, at the same time, it has a helix-promoting ability very similar to that of trifluoroethanol [15,16].

MATERIALS AND METHODS

Solid phase peptide synthesis and purification

Aβ-(1–42) was synthesized according to published methods using standard solid-phase synthesis techniques [17] with a Milligen 9050 synthesizer. Protected amino acids and chemicals were purchased from Bachem, Novabiochem or Fluka (Switzerland). The resin (4-hydroxymethylphenoxyacetic acid) on the polyethyleneglycol/polystyrene support, loaded with N^{α}-Fmoc-Ala (Fmoc-Ala-PAC-PEG-PS) was from Millipore (Waltham, MA, USA). Fmoc-Ala-PAC-PEG-PS resin (0.15 mmol·g^{-1}, 1 g) was treated with piperidine (20%) in dimethylformamide and linked with N^{α}-Fmoc-Ile (eightfold excess), *via* its pentafluorophenyl active ester. All the other N^{α}-Fmoc amino acids pentafluorophenyl active ester were sequentially coupled to the growing peptide chain and the coupling reaction time was 1 h. To optimize the synthesis, after each acylation step, we adopted a capping protocol with *N*-(2-chlorobenzyloxycarbonyloxy) succinimide as described [18]. Piperidine (20%) in dimethylformamide was used to remove the Fmoc group at all steps. After deprotection of the last N^{α}-Fmoc group, the peptide resin was washed with methanol and dried *in vacuo* to yield the protected Aβ-(1–42)-PAC-PEG-PS-Resin. The protected peptide-resin was treated with trifluoroacetic acid/H_2O/phenol/ethanedithiol/thioanisole (reagent K) (82.5 : 5 : 5 : 2.5 : 5, v/v/v/v) 10 mL per 1 g of resin at room temperature for 3 h [19]. After filtration of the exhausted resin, the solvent was concentrated *in vacuo* and the residue triturated with ether. The crude peptide was purified by high performance liquid chromatography using a Polymer Laboratories PLRP-S polymer-based reversed-phase column. The column was maintained at 45 °C and perfused at a flow rate of 1 mL·min^{-1} with a mobile phase containing solvent A (5 mM ammonium acetate, pH 8 in 5% acetonitrile), and a linear gradient from 0 to 20% of solvent B (5 mM ammonium acetate, pH 8 in 90% acetonitrile) in 25 min was adopted for the elution of the peptide. The fraction containing the pure peptide was lyophilized twice and the purity assessed by a MALDI-TOF analysis using a Hewlett Packard G2025A LD-TOF system mass spectrometer and α-cyano-4-hydroxycinnamic acid as matrix.

Sample preparation

It has been shown that a trifluoroacetic acid pretreatment renders Aβ easily soluble in aqueous solutions and in organic solvents; the trifluoroacetic acid treated Aβ exhibits the properties of monomeric, random coil structures and lacks preaggregated material [20]. Thus, in order to ensure sample reproducibility and removal of aggregated states which can be present, dry peptide was pretreated with neat trifluoroacetic acid for 3 h, followed by 10-fold dilution with milliQ water and lyophilization. This procedure was adopted for all CD and NMR samples immediately before dissolution in the appropriate solvent.

Circular dichroism spectroscopy

Circular dichroism (CD) measurements were performed on a JASCO J-715 spectropolarimeter equipped with a thermostated cell holder, using a quartz cell of 1.0-mm path length. Spectra were collected over the wavelength range 260–190 nm with a bandwidth of 2.0 nm and a time constant of 8.0 s, and corrected for the contribution of the buffer. In order to prevent peptide aggregation, which tends to occur when water is added directly, a prescored amount of trifluoroacetic acid-treated peptide was dissolved in 120 μL of HFIP and 160 μL of an appropriate HFIP/water mixture were added cautiously, to give a final peptide concentration of approximately 80 μM and a water content between 0 and 50% by volume. Unless otherwise stated, the temperature was 25 °C.

For estimation of secondary structure content, CD spectra were analyzed by a linear combination fit using the reference data of Greenfield and Fasman [21].

NMR spectroscopy

Samples for NMR spectroscopy were prepared by dissolving approximately 4 mg of trifluoroacetic acid-treated peptide in 200 μL of d_2-HFIP, followed by dilution with 300 μL of d_2-HFIP/H_2O (or d_2-HFIP/D_2O), 2 : 1 v/v. This results in a final HFIP/water ratio of 80 : 20 v/v,

corresponding to a water molar fraction of 0.60. The actual peptide concentration (approximately 2 mM) was checked before and after each measurement by UV absorbance, using an estimated extinction coefficient of 1280 $M^{-1}\cdot cm^{-1}$ at 280 nm.

NMR spectra were recorded on a Bruker DRX-600 spectrometer. One-dimensional spectra were recorded in the Fourier mode with quadrature detection and the water signal was suppressed by low-power selective irradiation. Two-dimensional COSY [22], TOCSY [23] and NOESY [24] experiments were collected in the phase-sensitive mode using quadrature detection in ω_1 by time-proportional phase increase of the initial pulse [25]. Typical data sizes were 2048 addresses in t_2 and 512 equidistant t_1 values. A mixing time of 80 ms was used for the TOCSY experiments. NOESY experiments were run at 300 K with mixing times in the range of 80–200 ms. The data were transformed with NMRPIPE [26] and analyzed with NMRVIEW [27]. Before Fourier transformation, the time domain data were multiplied by shifted sine functions (COSY) or lorentz-to-gauss windows (NOESY, TOCSY) in the direct dimension, and by shifted sine or sine square functions in the indirect dimension. The chemical shifts were referenced to the residual HFIP signal at 3.88 p.p.m.

The assignment of chemical shifts was obtained by the usual approach described by Wüthrich [28], examining COSY, TOCSY and NOESY spectra; some ambiguities arising from signal overlaps were resolved by examining spectra acquired at different temperatures (290 and 310 K) or in a d_2-HFIP/D_2O mixture. The assignment of chemical shifts was brought to 87% completeness (100% complete for the backbone). NOE cross peaks (d_2-HFIP/H_2O and d_2-HFIP/D_2O spectra) were integrated with NMRView and were converted into upper distance bounds with the routine CALIBA of the program package DYANA [29]. After discarding redundant and duplicated constraints, the final list included 130 intraresidue and 283 interresidue (149 sequential and 134 medium range) constraints, which were used to generate an ensemble of 100 structures by the standard protocol of simulated annealing in torsion angle space implemented in DYANA (using 6000 steps). No dihedral angle restraints and no hydrogen bond restraints were applied. The best 20 structures, which had low values of the target functions (0.83–1.19 $Å^2$) and small residual violations (maximum violation = 0.38 Å), were refined by *in vacuo* minimization in the AMBER 1991 force field [30], using the program SANDER of the AMBER 6 suite [31]. To mimic the effect of solvent screening, all net charges were reduced to 20% of their real value, and moreover a distance-dependent dielectric constant ($\varepsilon = r$) was used. The cut-off for non–bonded interactions was 12 Å. At this stage, the protonation states of the amino acid side chains were chosen to correspond to a low pH value, on account of the fact that the peptide samples had been pretreated with trifluoroacetic acid (see above). The NMR-derived upper bounds were imposed as semiparabolic penalty functions, with force constants of 16 $kcal\cdot mol^{-1}\cdot Å^2$; the function was shifted to linear when the violation exceeded 0.5 Å. The best 10 structures after minimization had AMBER energies ranging from −441.4 to −391.1 $kcal\cdot mol^{-1}$, and were used to represent the structure of Aβ-(1–42).

The final structures were analyzed using the program MOLMOL [32].

RESULTS

In the search for conditions which allow structural studies of Aβ in a homogeneous, isotropic environment, we have examined the solubility and spectroscopic features of Aβ-(1–42) in a variety of media in different concentration and temperature conditions. Several organic solvents and mixtures of organic solvents with water, such as trifluoroethanol, trifluoroethanol/H_2O, hexafluoroacetone hydrate, hexafluoroacetone hydrate/H_2O, HFIP/H_2O, CH_3OH, dimethylsulfoxide, dimethylsulfoxide/H_2O, were tested. The solubility of Aβ-(1–42) in methanol is poor; in contrast, trifluoroethanol and mixtures of trifluoroethanol/H_2O are able to dissolve the peptide but after few hours a precipitate was observed. Hexafluoroacetone hydrate and hexafluoroacetone hydrate/water mixtures can also dissolve the peptide at millimolar concentrations, and the solutions were stable for weeks; however, NMR signals were broad and the quality of data acquired in these solvents didn't allow an easy interpretation. Dimethylsulfoxide and mixtures of dimethylsulfoxide/H_2O (containing up to 5% water) seemed to be suitable solvents for studying the structure in solution by NMR, thus an almost complete backbone assignment was performed. However, the analysis of NOESY spectra evidenced only the presence of sequential, short-range contacts, suggesting the absence of any preferential conformation.

In the end, we found that stable, mM solutions of Aβ-(1–42) can be prepared in HFIP/H_2O mixtures. Water content and temperature can be changed within fairly large ranges without peptide precipitation. HFIP was chosen in view of its solvent power and also its ability to stabilize helical structures. In fact, although HFIP is a polar molecule, it can solvate apolar surfaces with its strongly hydrophobic side chains; this feature has been aptly described by Rajan *et al.* as a Teflon coating that can surround a helix [16] in the case of a mixture of water and hexafluoroacetone hydrate, a mixture with properties very similar to those of aqueous mixtures of HFIP. CD measurements on Aβ-(1–42) have shown that in HFIP/H_2O mixtures, under optimal conditions, the helical content can be higher than in other solvent mixtures in which conformational studies have been reported, such as aqueous trifluoroethanol or SDS micelles (data not shown).

The solvent mixture composition we adopted for NMR was also optimized by CD. Figure 1 shows the molar ellipticity at 220 nm, which can be related to the α-helix content, as a function of water percentage in the mixture. The ellipticity increases with the water concentration, reaching a plateau at approximately 20% water. Correspondingly, the helix content, as estimated by standard linear combination fits of the spectra [21], increases from 54% in neat HFIP to approximately 82% at the plateau. The CD spectrum in the 80 : 20 mixture is essentially unchanged in the temperature range 10–45 °C (data not shown), suggesting a high conformational stability of Aβ-(1–42) in this solvent medium, which was then selected to perform a detailed conformational analysis by 2D NMR. Furthermore, the Aβ-(1–42) solution in aqueous HFIP was very stable, as there was no evidence of aggregation or precipitation and the NMR spectra did not change over several weeks. The quality of NMR data is shown in Fig. 2, which displays the low field region of a 600-MHz NOESY

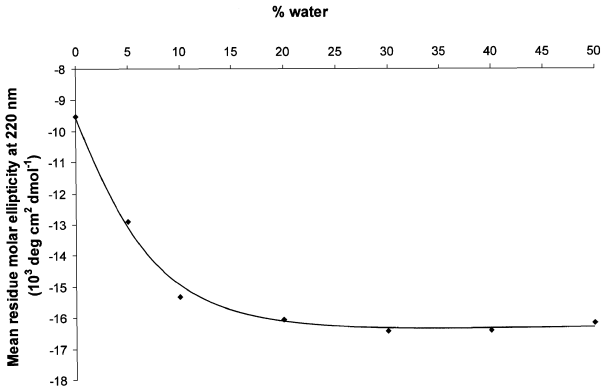

Fig. 1. Molar ellipticity at 220 nm of Aβ-(1–42) in HFIP/water mixtures as a function of water percentage at 25 °C.

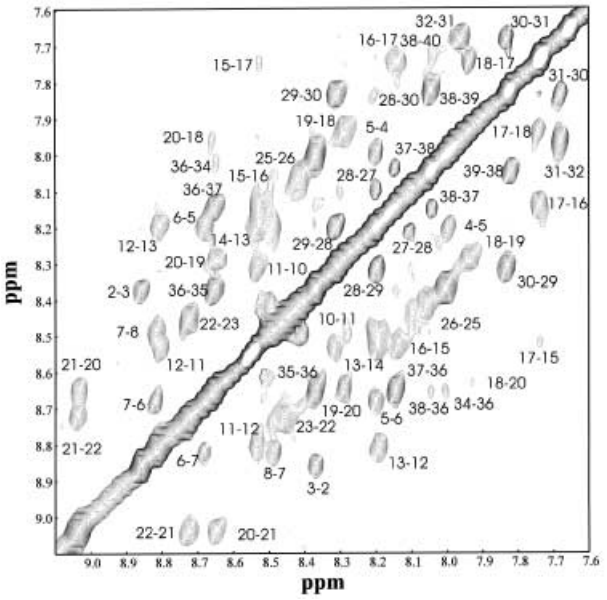

Fig. 2. Low field region of a 600-MHz NOESY spectrum of Aβ-(1–42) in HFIP/water at 300 K. The mixing time was 150 ms.

spectrum acquired at 300 K with a mixing time of 150 ms. The high number of NH–NH effects, summarized in Fig. 3, is consistent with the prevalent helical fold suggested by the CD data. At first sight, the NOE pattern could be interpreted as a good evidence of the presence of a single helical region encompassing residues 8–40. However, whereas sequential and medium range connectivities expected for helical regions, i.e. HN–HN (i, i + 1), Hα–HN (i, i + 3), Hα–Hβ (i, i + 3) and Hα–HN (i, i + 4), are present (or hidden by trivial spectral overlaps) along the whole stretch 8–40, the crucial contact between Ser26 Hα and Ala30 HN is absent. Moreover, Hα–HN (i, i + 1) contacts, typical of extended structures, are also rather strong in this region: taken together, these features can point to an enhanced flexibility or possibly a break in the helix.

Structure calculation by a standard DYANA protocol yielded a bundle of 20 structures with satisfactory values of the target function; after restrained minimization in the AMBER force field (Table 1), the best structures formed a tightly clustered family, consisting of two helical regions (residues 8–25 and 28–38, respectively), connected by a kink (Fig. 4). The first helix is very well defined, with a backbone RMSD of just 0.38 Å, while the second helix is interrupted in some structures at the level of the Ile32–Gly33 connection. Closer inspection of the kink region reveals the presence of a type I β-turn centred on residues 25–26, while residue 27 displays values of the backbone ϕ e ψ dihedrals around (−150°, 40°), i.e. in the 'additionally allowed' region of the Ramachandran map. Unconstrained minimization of the structures did not produce any major rearrangement in this region, which instead would be expected if the observed dihedrals were imposed by the influence of artifactual NMR restraints. Thus, the type I β-turn centred on residues 25–26

Table 1. Summary of residual constraint violations and energies. The force constants for the distance constraints were 16 kcal·mol^{-1}·Å^{-2}. The errors are given as ± SD.

Range, d (Å)	Average number of distance constraint violations
$0.1 < d <= 0.2$	26.9 ± 4.1
$0.2 < d <= 0.3$	9.7 ± 2.2
$0.3 < d <= 0.4$	1.6 ± 1.1
$0.4 < d <= 0.5$	0.7 ± 0.4
$0.5 < d$	0
Average maximum violation (Å)	0.43 ± 0.03

Energy term	Average AMBER energies (kcal·mol^{-1})
E (AMBER)	−415.7 ± 16.4
E (distance constraint)	25.5 ± 2.0
E (Van der Waals)	−159.6 ± 4.5
E (total)	−390.1 ± 17.6

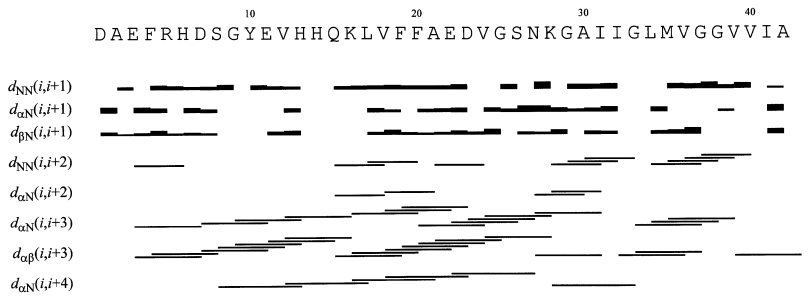

Fig. 3. Bar diagram showing the NOE connectivities observed for Aβ-(1–42) in HFIP/water 80 : 20 at 300 K. The thickness of lines is related to the strength of connectivities.

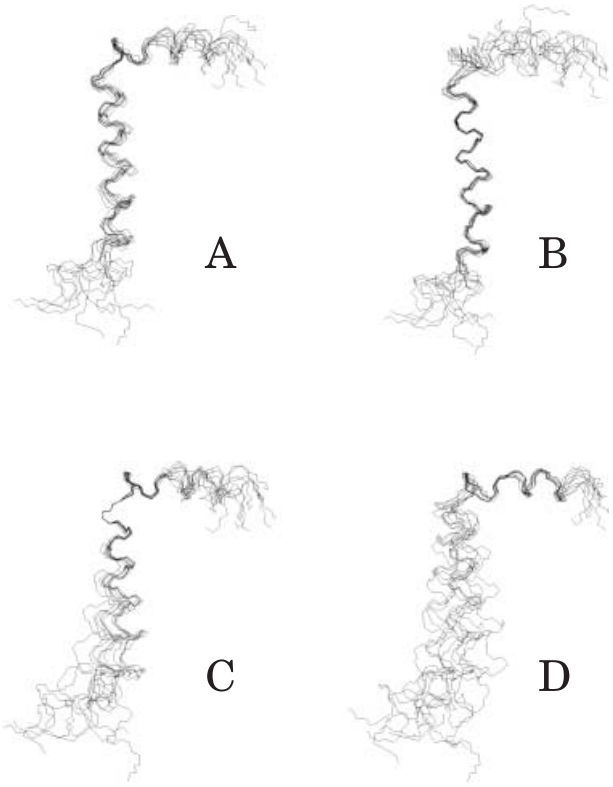

Fig. 4. Bundle of the best 10 structures of Aβ-(1–42) after AMBER minimization, superimposed for: (A) backbone atoms of residues 8–38 (RMSD = 0.86 Å); (B) backbone atoms of residues 8–25 (RMSD = 0.38 Å); (C) backbone atoms of residues 26–27 (RMSD = 0.048 Å); (D) backbone atoms of residues 28–38 (RMSD = 0.59 Å).

appears to be a genuine feature of the global structure of Aβ-(1–42).

At first sight, the shape of the molecule resulting from our structure determination is similar to other helical structures of full length Aβ, i.e. Aβ-(1–40) or Aβ-(1–42) [12–14]: however, a more detailed comparison reveals a number of significant differences. The structure of Aβ-(1–40) in trifluoroethanol/water mixture [14] displays two helices, over residues 15–22 and 30–35, separated by a 6-residues long disordered region. The remaining NMR studies on full length Aβ published to date have been carried out in SDS micelles. The structure of Aβ-(1–40) reported by Coles *et al.* [12] consists of a single helix from residue 15–36, with only a slight bend around residues 26–27; by contrast, the structure published by Shao *et al.* [13] is described in terms of two α-helices, 10–24 and 28–42, separated by a marked loop involving residues 25–27, with no significant difference found between Aβ-(1–40) and Aβ-(1–42). Thus, even in comparison with these SDS studies, the helical regions in our structure are longer and better defined; moreover, while an α-helix break is present more or less at the same position in all previous cases, we observe a well defined elbow-shaped structural element.

We believe that the regularity of our structure in comparison to those described in [12–14] is a direct consequence of an environment, which can simulate in some way the inner membrane, i.e. the lipid phase.

DISCUSSION

Conformational studies in aqueous solution of Aβ have been hampered by fast peptide aggregation, and only very recently some NMR investigation on small fragments [33,34], as well as on Aβ-(1–40)^{ox} [35], containing methionine sulfoxide at position 35, have been reported. All these studies, although referred to fragments of different length, with different oxidation states of Met35, and at different pH, suggest that in aqueous solution the peptide can be described as a random coil, with only a small population of local nonrandom structures. Overall, these data indicate that bulk water is not suitable for high resolution conformational analysis of Aβ. Moreover several structural investigations in different solvents, reviewed in [12], suggest that *in vitro* the secondary structure of Aβ is strongly dependent on experimental conditions. This is a typical feature of small and medium size peptides, but in the case of Aβ the conformational flexibility is particularly interesting, as it can be related to its biological activity. The choice of the solvent is crucial not only to overcome the solubility problem, but also to try to simulate in some aspects the physico-chemical

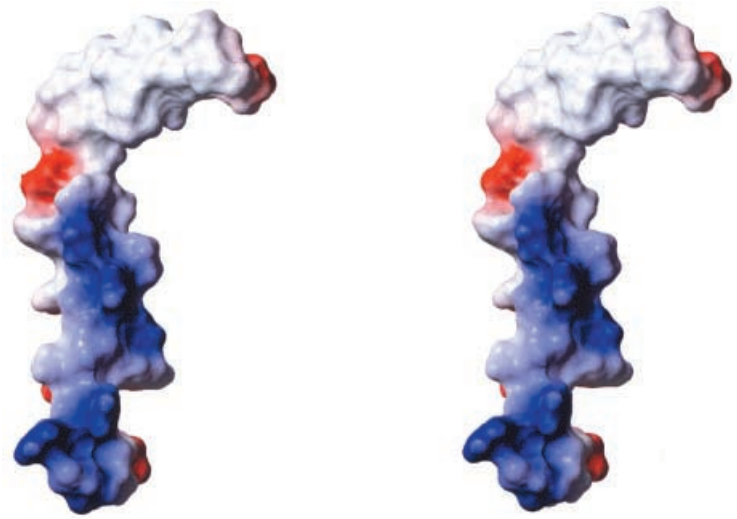

Fig. 5. Stereo view of the lowest energy structure colored according to the electrostatic potential.

features of the different environments to which the peptide is exposed *in vivo*. In particular, if the peptide exerts its toxicity by membrane disruption, it is important to check whether Aβ-(1–42) can assume a regular ordered conformation in an environment with properties similar to those of the lipid phase of the membrane, which promotes the formation of short-range H-bonds inducing helical structures.

The structural characterization of a monomeric, soluble form of Aβ-(1–42) in isotropic media is necessary not only to shed some light on the steps involved in the fibrillogenesis, but, most of all, to evaluate the role of Aβ-(1–42) in the interaction with the membrane.

The structure of Aβ-(1–42) found in aqueous hexafluoroisopropanol, a medium that mimics the lipidic environment of membranes, is boomerang-shaped. It is interesting to note that the second helix (residues 28–38) corresponds to the transmembrane region of APP, and has the typical amino acid composition of transmembrane helices, i.e. small (Gly and Ala) and hydrophobic (Ile, Leu, Met and Val) residues [36]. The only charged residue along this sequence is Lys28, i.e. at the N-terminal end of the helix.

A contact surface representation of the lowest energy structure colour-coded according to the electrostatic potential (Fig. 5) shows the presence of a wide positive region within the first helical region. Interestingly, if one positions this surface facing the charged phospholipids of a membrane, the relative orientation of the second helix is such that it can insert into the membrane. It is interesting to note that the structure we find for Aβ-(1–42) is in very good agreement with a theoretical model proposed for membrane bound Aβ-(1–40) [37]; indeed, between Lys16 and Val40 the two structures are almost identical, including the turn involving Gly25, Ser26 and Asn27. Different packing schemes giving rise to membrane channels have been proposed for this structure [37].

The overall shape of Aβ-(1–42) is strongly reminiscent of the structure of the fusion domain of influenza hemagglutinin (HA_fd), recently determined in detergent micelles [38] (Fig. 6A and B). Even more significant is the finding that the sequences of the C-terminal part of Aβ-(1–42) and that of HA_fd share indeed a high similarity (Fig. 6C) dictated essentially by the presence of similarly spaced glycine residues, which are considered essential for a good insertion into the membrane and are also frequently involved in membrane protein dimerization [39]. The role of these residues is also evidenced by a similar distribution on the surface of the structures. The breaks in the helix-break-helix motif (indicated by boxed residues), although at nearby positions in the two sequences, are not coincident; however, both structures feature a hydrophobic patch in the inner region of the bent, made up by a cluster of 4/5 aliphatic and/or aromatic side-chains. These findings lend strong support to the hypothesis that the peptide neurotoxicity is due to a membrane-poration process [10,11]. This view is also confirmed by the very recent observation that *in vitro* Aβ-(1–40) can insert into a lipid bilayer just by its C-terminus [40]; moreover, upon insertion a conformational transition generating approximately 60% α-helix has been evidenced. By contrast, it has been proposed that HA_fd inserts both helical stretches into the membrane [38]. Accordingly, it is possible that the mechanism of membrane interaction and destabilization is different in the case of Aβ,

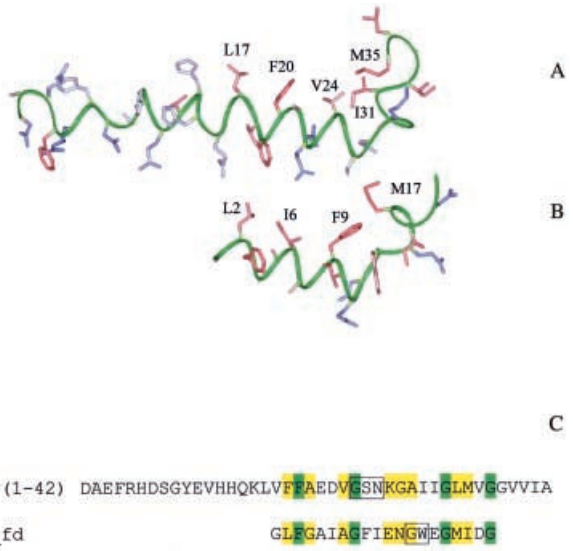

Fig. 6. Comparison of the shapes of the lowest energy structure of HA_fd (A) and of the 1–35 region of Aβ-(1–42) (B). Residue side chains are colored according to their hydrophobic character (high = red, low = blue). The sequences of the two peptides, aligned with CLUSTALX [42], are shown in panel (C). Identical residues are reported in green, conserved or semiconserved in yellow.

but it is fair to say that the similarity with the fusion domain of a virus is strongly suggestive of membrane disruption. The recent observation of a strong synergism between Aβ and several viruses at the stage of attachment or entry into the cell lends further support to this hypothesis [41].

Coordinates

Coordinates have been deposited in the Protein Data Bank. The access code is 1IYT.

ACKNOWLEDGMENTS

This work was supported by a grant from Regione Campania (legge regionale 41/94), Italy.

REFERENCES

1. Iversen, L.L., Mortishire-Smith, R.J., Pollack, S.J. & Shearman, M.S. (1995) The toxicity *in vitro* of beta-amyloid protein. *Biochem. J.* **311**, 1–16.
2. Jarrett, J.T., Berger, E.P. & Lansbury, P.T. Jr (1993) The C-terminus of the beta protein is critical in amyloidogenesis. *Ann. NY Acad. Sci.* **695**, 144–148.
3. Selkoe, D.J. (1994) Normal and abnormal biology of the β-amyloid precursor protein. *Annu. Rev. Neurosci.* **17**, 489–517.
4. Masters, C.L., Simms, G., Weinman, N.A., Multhaup, G., McDonald, B.L. & Beyreuther, K. (1985) Amyloid plaque core protein in Alzheimer disease and Down syndrome. *Proc. Natl Acad. Sci. USA* **82**, 4245–4249.
5. Esler, W.P. & Wolfe, M.S. (2001) A portrait of Alzheimer secretases-new features and familiar faces. *Science* **293**, 1449–1454.
6. Lichtenthaler, S.F., Beher, D., Grimm, H.S., Wang, R., Shearman, M.S., Masters, C.L. & Beyreuther, K. (2002) The intramembrane cleavage site of the amyloid precursor protein depends on the length of its transmembrane domain. *Proc. Natl Acad. Sci. USA* **99**, 1365–1370.

7. Lichtenthaler, S.F., Wang, R., Grimm, H., Uljon, S.N., Masters, C.L. & Beyreuther, K. (1999) Mechanism of the cleavage specificity of Alzheimer's disease gamma-secretase identified by phenylalanine-scanning mutagenesis of the transmembrane domain of the amyloid precursor protein. *Proc. Natl Acad. Sci. USA* **96**, 3053–3058.
8. Koo, E.H., Lansbury, P.T. & Kelly, J.W. (1999) Amyloid diseases: abnormal protein aggregation in neurodegeneration. *Proc. Natl Acad. Sci. USA* **96**, 9989–9990.
9. Rhee, S.K., Quist, A.P. & Lal, R. (1998) Amyloid beta protein-(1–42) forms calcium-permeable, Zn^{2+}-sensitive channel. *J. Biol. Chem.* **273**, 13379–13382.
10. Lin, H., Bhatia, R. & Lal, R. (2001) Amyloid beta protein forms ion channels: implications for Alzheimer's disease pathophysiology. *FASEB J.* **15**, 2433–2444.
11. Kirkitadze, M.D., Condron, M.M. & Teplow, D.B. (2001) Identification and characterization of key kinetic intermediates in amyloid β-protein fibrillogenesis. *J. Mol. Biol.* **312**, 1103–1119.
12. Coles, M., Bicknell, W., Watson, A.A., Fairlie, D.P. & Craik, D.J. (1998) Solution structure of amyloid β-peptide (1–40) in a water-micelle environment. Is the membrane-spanning domain where we think it is? *Biochem.* **37**, 11064–11077.
13. Shao, H., Jao, S., Ma, K. & Zagorski, M.G. (1999) Solution structures of micelle-bound amyloid β-(1–40) and β-(1–42) peptides of Alzheimer's disease. *J. Mol. Biol.* **285**, 755–773.
14. Sticht, H., Bayer, P., Willbold, D., Dames, S., Hilbich, C., Beyreuther, K., Frank, R.W. & Rosch, P. (1995) Structure of amyloid A4-(1–40) -peptide of Alzheimer's disease. *Eur. J. Biochem.* **233**, 293–298.
15. Bhattacharjya, S., Venkatraman, J., Kumar, A. & Balaram, P. (1999) Fluoroalcohols as structure modifiers in peptides and proteins: hexafluoroacetone hydrate stabilizes a helical conformation of melittin at low pH. *J. Peptide Res.* **54**, 100–111.
16. Rajan, R., Awasthi, S.K., Bhattachajya, S. & Balaram, P. (1997) 'Teflon-coated peptides': hexafluoroacetone trihydrate as a structure stabilizer for peptides. *Biopolymers* **42**, 125–128.
17. Atherton, E. & Sheppard, R.C. (1989) *Solid Phase Peptide Synthesis*, (D. Rickwood & B.D. Hames, eds.) IRL Press, Oxford.
18. Ball, H.L. & Mascagni, P. (1996) Chemical synthesis and purification of proteins: a methodology. *Int. J. Pept. Protein Res.* **48**, 31–47.
19. King, D.S., Fields, C.G. & Fields, G.B. (1990) A cleavage method which minimizes side reactions following Fmoc solid phase peptide synthesis. *Int. J. Pept. Protein Res.* **36**, 255–266.
20. Jao, S.C., Ma, K., Talafous, J., Orlando, R. & Zagorski, M.G. (1997) Trifluoroacetic acid pretreatment reproducibly disaggregates the amyloid β-peptide. *Int. J. Exp. Clin. Invest.* **4**, 240–252.
21. Greenfield, N. & Fasman, G.D. (1969) Computed circular dichroism spectra for the evaluation of protein conformation. *Biochemistry* **8**, 4108–4116.
22. Aue, W.P., Bartholdi, E. & Ernst, R.R. (1976) Two-dimensional spectroscopy. Application to nuclear magnetic resonance. *J. Chem. Phys.* **64**, 2229–2246.
23. Bax, A. & Davis, D.G. (1985) Practical aspect of two-dimensional transverse NOE spectroscopy. *J. Magn. Reson.* **65**, 335–360.
24. Jeener, J., Meyer, B.H., Bachman, P. & Ernst, R.R. (1979) Investigation of exchange processes by two-dimensional NMR spectroscopy. *J. Chem. Phys.* **71**, 4546–4553.
25. Marion, D. & Wüthrich, K. (1983) Application of phase sensitive two-dimensional correlated spectroscopy (COSY) for measurements of ^{1}H-^{1}H spin-spin coupling costants in proteins. *Biochem. Biophys. Res. Comm.* **113**, 967–971.
26. Delaglio, F., Grzesiek, S., Vuister, G., Zhu, G., Pfeifer, J. & Bax, A. (1995) NMRPipe: a multidimensional spectral processing system based on UNIX pipes. *J. Biomol. NMR* **6**, 277–293.
27. Johnson, B.A. & Blevins, R.A. (1994) NMRView: a computer program for the visualization and analysis of NMR data. *J. Biomol. NMR* **4**, 603–614.
28. Wüthrich, K. (1986) *NMR of Proteins and Nucleic Acids*, John Wiley & Sons, New York.
29. Güntert, P., Mumenthaler, C. & Wüthrich, K. (1997) Torsion angle dynamics for NMR structure calculation with the new program DYANA. *J. Mol. Biol.* **273**, 283–298.
30. Weiner, S.J., Kollman, P.A., Nguyen, D.T. & Case, D.A. (1986) An all atom force field for simulations of proteins and nucleic acids. *J. Comp. Chem.* **7**, 230–252.
31. Pearlman, D.A., Case, D.A., Caldwell, J.W., Ross, W.S., Cheatham, T.E. III, DeBolt, S., Ferguson, D., Seibel, G. & Kollman, P.A. (1995) AMBER, a package of computer programs for applying molecular mechanics, normal mode analysis, molecular dynamics and free energy calculations to simulate the structural and energetic properties of molecules. *Comp. Phys. Commun.* **91**, 1–41.
32. Koradi, R., Billeter, M. & Wüthrich, K. (1996) MOLMOL: a program for display and analysis of macromolecular structures. *J. Mol. Graph.* **14**, 51–55.
33. Jarvet, J., Damberg, P., Bodell, K., Eriksson, L.E.G. & Gräslund, A. (2000) Reversible random coil to β-sheet transition and the early stage of aggregation of the Aβ (12–28) fragment from the Alzheimer. *J. Am. Chem. Soc.* **122**, 4261–4268.
34. Zhang, S., Iwata, K., Lachenmann, M.J., Peng, J.W., Li, S., Stimson, R.R., Lu, Y.A., Felix, A.M., Maggio, J.E. & Lee, J.P. (2000) The Alzheimer's peptide Aβ adopts a collapsed coil structure in water. *J. Struct. Biol.* **130**, 130–141.
35. Riek, R., Güntert, P., Döbell, H., Wipf, B. & Wüthrich, K. (2001) NMR studies in aqueous solution fail to identify significant conformational differences between the monomeric forms of two Alzheimer peptides with widely different plaque-competence, Aβ (1–40) ^{ox} and Aβ (1–42) ^{ox}. *Eur. J. Biochem.* **268**, 5930–5936.
36. Eilers, M., Shekar, S.C., Shieh, T., Smith, S.O. & Fleming, P.J. (2000) Internal packing of helical membrane proteins. *Proc. Natl Acad. Sci. USA* **97**, 5796–5801.
37. Durell, S.R., Guy, R., Arispe, N., Rojas, E. & Pollard, B. (1994) Theoretical models of the ion channel structure of amyloid β-protein. *Biophys. J.* **67**, 2137–2145.
38. Han, X., Bushweller, J.H., Cafiso, D.S. & Tamm, L.K. (2001) Membrane structure and fusion-triggering conformational change of the fusion domain from influenza hemagglutinin. *Nat. Struct. Biol.* **8**, 715–720.
39. Javadpour, M.M., Eilers, M., Groesbeek, M. & Smith, S.O. (1999) Helix packing in polytopic membrane proteins: role of glycine in transmembrane helix association. *Biophys. J.* **77**, 1609–1618.
40. Ji, S.R., Wu, Y. & Sui, S. (2002) Cholesterol is an important factor affecting the membrane insertion of β-amyloid peptide (Aβ1–40), which may potentially inhibit the fibril formation. *J. Biol. Chem.* **277**, 6273–6279.
41. Wojtowicz, W.M., Farzan, M., Joyal, J.L., Carter, K., Babcock, G.J., Israel, D.I., Sodroski, J. & Mirzabekov, T. (2002) Stimulation of enveloped virus infection by beta-amyloid fibrils. *J. Biol. Chem.* in press.
42. Thompson, J.D., Gibson, T.J., Plewniak, F., Jeanmougin, F. & Higgins, D.G. (1997) The CLUSTAL_X windows interface: flexible strategies for multiple sequence alignment aided by quality analysis tools. *Nucleic Acids Res.* **24**, 4876–4882.